



## Novel Scintillation Detectors for Prompt Fission $\gamma$ -Ray Measurements

Downloaded from: <https://research.chalmers.se>, 2025-12-04 23:39 UTC

Citation for the original published paper (version of record):

Billnert, R., Andreotti, E., Hambsch, F. et al (2012). Novel Scintillation Detectors for Prompt Fission  $\gamma$ -Ray Measurements. Physics Procedia, 31: 29-34. <http://dx.doi.org/10.1016/j.phpro.2012.04.005>

N.B. When citing this work, cite the original published paper.

GAMMA-1 Emission of Prompt Gamma-Rays in Fission and Related Topics

## Novel Scintillation Detectors for Prompt Fission $\gamma$ -Ray Measurements

R. Billnert<sup>a,b,\*</sup>, E. Andreotti<sup>a</sup>, F.-J. Hambsch<sup>a</sup>, M. Hult<sup>a</sup>, J. Karlsson<sup>c</sup>,  
G. Marissens<sup>a</sup>, A. Oberstedt<sup>b,c</sup>, S. Oberstedt<sup>a</sup>

<sup>a</sup>European Commission, DG Joint Research Centre (IRMM), B-2440 Geel, Belgium

<sup>b</sup>Fundamental Fysik, Chalmers Tekniska Högskola, S-41296 Göteborg, Sweden

<sup>c</sup>Akademi för Naturvetenskap och Teknik, Örebro Universitet, S-70182 Örebro, Sweden

---

### Abstract

In this work we present first results from measurements of prompt fission  $\gamma$ -rays from the spontaneous fission in  $^{252}\text{Cf}$ . New and accurate data on corresponding  $\gamma$ -rays from the reactions  $^{235}\text{U}(\text{n}_{\text{th}},\text{f})$  and  $^{239}\text{Pu}(\text{n}_{\text{th}},\text{f})$  are highly demanded for the modeling of new Generation-IV nuclear reactor systems. For these experiments we employed scintillation detectors made out of new materials ( $\text{LaBr}_3$ ,  $\text{LaCl}_3$  and  $\text{CeBr}_3$ ), whose properties were necessary to know in order to obtain reliable results. Hence, we have characterized these detectors. In all the important properties these detectors outshine sodium-iodine detectors that were used in the 1970s, when the existing data had been acquired. Our finding is that the new generation of scintillation detectors is indeed promising, as far as an improved precision of the demanded data is concerned.

© 2012 Published by Elsevier B.V. Selection and/or peer-review under responsibility of Institute for Reference Materials and Measurements. Open access under [CC BY-NC-ND license](#).

**Keywords:** Prompt fission  $\gamma$ -rays;  $^{252}\text{Cf}$ ; Lanthanum-Chloride; Cerium-Bromide; Energy resolution; Timing resolution; Intrinsic peak efficiency

---

---

\* Corresponding author. Tel.: +32 (0)14 573 014; fax: +32 (0)14 571 376.

E-mail address: [Robert.Billnert@ec.europa.eu](mailto:Robert.Billnert@ec.europa.eu).

## 1. Introduction

One of the major challenges with the modeling of Gen-IV fast nuclear reactors is the assessment of  $\gamma$ -heating from the fission process, which accounts for about 10% of the total energy released in fission [1]. Apparently, those modern designs require  $\gamma$ -heating to be known with an uncertainty as low as 7.5% ( $1\sigma$ ), but available data that were actually measured already in the early 1970's, seems to underestimate  $\gamma$ -heating with up to 28%. This deviation is basically due to difficulties to estimate the impact prompt fission  $\gamma$ -rays, which amount around 40% of all  $\gamma$ -rays. Hence, the OECD has requested updated data on two of the main fuel isotopes  $^{235}\text{U}$  and  $^{239}\text{Pu}$  [2].

A common way to separate prompt fission  $\gamma$ -rays experimentally from those produced in neutron-induced reactions is to measure them in coincidence with the fission fragments, and then evaluate their time-of-flight between source and detector. In order to apply this method it is desired to use detectors with a timing resolution as good as possible. Other important properties of the used  $\gamma$ -detectors are good energy resolution in order to determine the precise shape of the energy spectrum and therefore minimize the uncertainty in average energy, and a high full-peak efficiency in order to reduce statistical uncertainties in determining  $\gamma$ -ray multiplicities. In the early 1970's sodium-iodine (NaI) detectors were used to measure prompt fission  $\gamma$ -rays. However, those detectors have limited capabilities in regard of energy and timing resolution, but they were the best detectors available at that time. In the last few years there has been an increased interest in the development of new scintillation detectors that provide better energy as well as timing resolution compared to NaI detectors. These resulted in lanthanide-halide detectors, such as lanthanum-chloride ( $\text{LaCl}_3$ ) and lanthanum-bromide ( $\text{LaBr}_3$ ) detectors, as well as the very recently developed cerium-bromide ( $\text{CeBr}_3$ ) detectors. They all show great promise to be able to improve the present data on prompt fission  $\gamma$ -rays, since all important properties are superior to those of NaI detectors.

In this work we will present our results from the characterization of two of these detectors,  $\text{LaCl}_3$  and  $\text{CeBr}_3$  detectors, as well as present our first fission  $\gamma$ -ray spectra for spontaneous fission from  $^{252}\text{Cf}$  for both a  $\text{LaCl}_3$  and a  $\text{CeBr}_3$  detector as well as with a  $\text{LaBr}_3$  detector.

## 2. Experiments

### 2.1. Detector characterization

The detectors characterized in this work are three 1.5 in.  $\times$  1.5 in.  $\text{LaCl}_3$  detectors, one 1 in.  $\times$  1 in.  $\text{CeBr}_3$  detector as well as one 1 in.  $\times$  2 in.  $\text{CeBr}_3$  detector. All three detector types were manufactured by SCIONIX [3] and coupled to Photonis XP5200 or Photonis XP642B01 photomultiplier tubes (PMT), which provide only one output signal from the anode, so we had to split the signal using a 1 k $\Omega$  splitter to match the impedance of the amplifier. By this it was possible to measure both the timing and the energy signal simultaneously in a coincidence set-up. One output was connected to a delay-line amplifier (Ortec 460) to measure the energy properties, while the other output was fed into a timing filter amplifier (Ortec 476), and then to a constant fraction module to determine the timing characteristics. The information from both signals was then digitized with Canberra 8715 ADCs, before passed on to the data acquisition system DAQ-2000 [4].

The presence of intrinsic activity in lanthanum-halide detectors due to naturally occurring radioactive contaminants had already been established in lanthanum-halide detectors [5-9], and reported as well for cerium-bromide crystals [10], which however came from another manufacturer than our one. Therefore,

we moved the detector to the underground laboratory HADES [11], which is located 225 m below ground on the premises of the Belgian Nuclear Research Centre SCK•CEN. The sand-clay overburden assures a muon flux reduction of about 5000. It turned out that the intrinsic activity of our CeBr<sub>3</sub> detector is much less than we usually find in lanthanum halide detectors [12], and also less than reported in Ref. [10] for a similar detector.

## 2.2. Prompt fission $\gamma$ -ray measurements

In order to measure prompt fission  $\gamma$ -rays, the signals from the scintillation detectors were taken in coincidence with the instant of fission events. The CeBr<sub>3</sub> and LaBr<sub>3</sub> detectors were set up facing a low mass fission chamber, containing <sup>252</sup>Cf as spontaneous fission source. The LaCl<sub>3</sub> detector was used in conjunction with a radiation-hard artificial diamond detector providing the fission trigger, placed inside a fission chamber again with a <sup>252</sup>Cf sample. By plotting time-of-flight versus pulse height for each photon detected by the scintillation detectors prompt fission  $\gamma$ -rays are easily distinguished from  $\gamma$ -rays produced in other reactions [5].

## 3. Results and discussions

### 3.1. Detector characterization

In this section we give a short description of the different steps in the characterization of the detectors and present the results. More detailed information for the LaCl<sub>3</sub> and the CeBr<sub>3</sub> detectors may be found in Refs. [5,12], respectively.

#### 3.1.1. LaCl<sub>3</sub> detectors

In order to determine the energy resolution for these detectors, we used <sup>22</sup>Na, <sup>137</sup>Cs, <sup>60</sup>Co and <sup>232</sup>Th sources to cover the energy range of 239 to 2615 keV. The energy resolution was then defined as the Full-Width-of-Half-Maximum (FWHM) of the Gaussian fitted to the full-energy peak relative to the peak energy. This was plotted against the peak energy and fitted with a power function according to Ref. [13]. The results are shown in Fig. 1 and can be described by

$$FWHM(\%) = 102.4 \times E^{-0.5001}, \quad (1)$$

which corresponds very well with the expected  $E^{-1/2}$  behavior and gives an energy resolution of 4% for the 661.67 keV line from the decay of <sup>137</sup>Cs. For comparison corresponding data for 3 in.  $\times$  3 in. NaI detector is shown as well.

The intrinsic full peak efficiency was determined by using a set of calibration sources with known activity, placed at a certain distance. The detected number of events in the full-energy peak was compared to the activity of the sources, taking into account the geometrical efficiency with an equation from Ref. [14]. The found values as a function of  $\gamma$ -energy from 122 to 2614.5 keV are shown in Fig. 2, again with the corresponding values for a 3 in.  $\times$  3 in. NaI detector as reference.

The timing resolution was determined by measuring two coincident  $\gamma$ -rays from <sup>22</sup>Na and <sup>60</sup>Co sources with two detectors in a coincidence set-up. The detectors were located with an angle of 45° between them, to diminish the very potent 511 keV annihilation photons from <sup>22</sup>Na as well as crosstalk between the

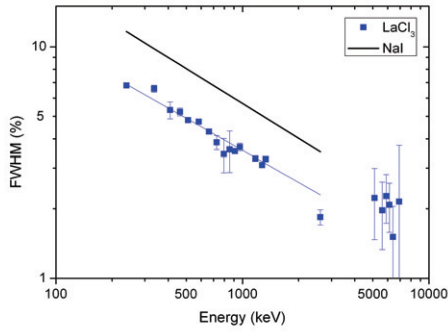


Figure 1: Measured energy resolution for  $\gamma$ -rays as a function of energy for a 1.5 in.  $\times$  1.5 in.  $\text{LaCl}_3$  detector. For comparison corresponding data for a 3 in.  $\times$  3 in. NaI detector is shown as well.

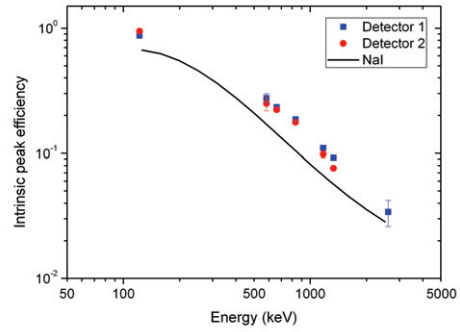


Figure 2: Intrinsic full peak efficiency as a function of  $\gamma$ -energy for two  $\text{LaCl}_3$  detectors, together with values for a 3 in.  $\times$  3 in. NaI detector.

detectors. To investigate the pulse-height dependent jitter of the constant fraction module, we applied different low-threshold cut off energies. To determine the intrinsic timing resolution from the measured coincidence distribution, we use the following formula,

$$T_{\text{coinc}}^2 = t_1^2 + t_2^2, \quad (2)$$

where  $T_{\text{coinc}}$  is the FWHM from the Gaussian fit over the measured timing distribution, and  $t_1$  and  $t_2$  are the intrinsic timing resolution from each detector. To solve this equation with two unknown variables we measured the three different  $\text{LaCl}_3$  detectors in the three possible pair configurations, and from that we deduced the intrinsic timing resolution for each detector. Our best detector has an intrinsic timing resolution of 763(6) ps and 352(11) ps for a threshold of 100 keV and 1100 keV respectively.

### 3.1.2. $\text{CeBr}_3$ detectors

The energy resolution for the 1 in.  $\times$  1 in.  $\text{CeBr}_3$  detector was determined with the same setup as was used for the  $\text{LaCl}_3$  detector. The equation equivalent to eq. 1 for this detector is:

$$FWHM(\%) = 113 \times E^{-0.5008}, \quad (3)$$

which also corresponds very well with the expected  $E^{-1/2}$  dependence with energy. The measured value for the 661.67 keV line from  $^{137}\text{Cs}$  was 4.4% for both this detector and for the 1 in.  $\times$  2 in.  $\text{CeBr}_3$  detector.

For the intrinsic efficiency we did not have calibration sources with known activity during the time of measurement. Therefore, we used one  $\text{LaCl}_3$  detector with known efficiency in the same set-up as described before to determine the source strength. The results from this measurement can be seen in Fig. 4, the results from the best  $\text{LaCl}_3$  detector are included for comparison.

For the timing resolution we measured the detector in coincidence with the best  $\text{LaCl}_3$  detector, since the exact intrinsic timing resolution of this detector was known. As before we used  $^{22}\text{Na}$  and  $^{60}\text{Co}$  as sources and we applied different low energy thresholds. For a threshold energy of 100 keV the intrinsic timing resolution was 780(7) ps and 760(10) ps for the 1 in.  $\times$  1 in. and the 1 in.  $\times$  2 in.  $\text{CeBr}_3$  detector,

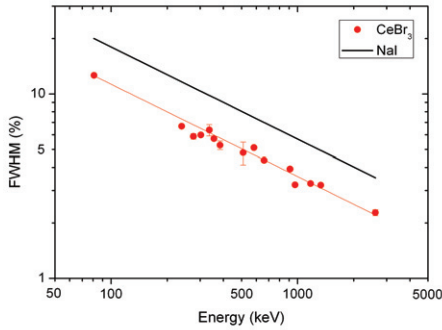


Figure 3: Measured energy resolution for  $\gamma$ -rays as a function of energy for a 1 in.  $\times$  1 in.  $\text{CeBr}_3$  detector. For comparison corresponding data for a 3 in.  $\times$  3 in.  $\text{NaI}$  detector is shown too.

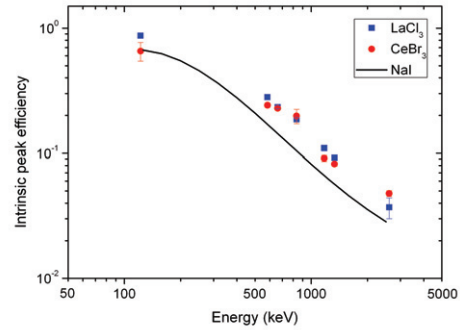


Figure 4: Intrinsic full peak efficiency as a function of  $\gamma$ -energy for a 1 in.  $\times$  1 in.  $\text{CeBr}_3$  detector, compared to a 1.5 in.  $\times$  1.5 in.  $\text{LaCl}_3$  detector as well as a 3 in.  $\times$  3 in.  $\text{NaI}$  detector.

respectively. For a threshold energy of 1100 keV we measured an intrinsic timing resolution of 326(7) ps and 400(16) ps for the respective detector.

To determine if the  $\text{CeBr}_3$  detectors contained any contamination, we transported them to the underground laboratory HADES. There the two detectors were measured by a high purity germanium detector. The results from this was that the maximum amount of background contamination in the detectors was 0.08 Bq/cm<sup>3</sup>/s for the 1 in.  $\times$  1 in. detector and 0.03 Bq/cm<sup>3</sup>/s for the 1 in.  $\times$  2 in. over the energy range of 0 to 3 MeV. This leads to the conclusion that most of this contamination is located in the PMT.

### 3.2. Results from first prompt fission $\gamma$ -ray measurement

Figure 5 show our measured prompt fission  $\gamma$ -ray spectra taken with all three different detector types, the source in all cases are spontaneous fission from  $^{252}\text{Cf}$ . The data has been treated with the same background suppress technique as in Ref. [5], and is, therefore, devoid of both intrinsic activity as well as  $\gamma$ -rays from the environment. These spectra need to be unfolded with the corresponding detector's

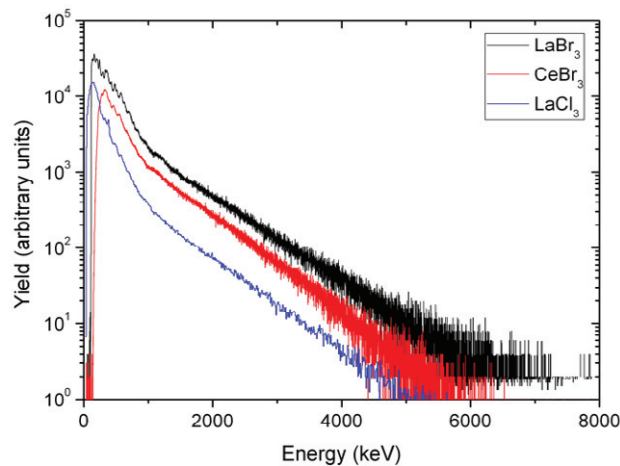


Figure 5: Prompt fission  $\gamma$ -ray spectra taken with 2 in.  $\times$  2 in.  $\text{LaBr}_3$ , 1 in.  $\times$  2 in.  $\text{CeBr}_3$  and a 1.5 in.  $\times$  1.5 in.  $\text{LaCl}_3$  detector. The source was spontaneous fission from  $^{252}\text{Cf}$ . The yield is arbitrary, but we can see that all three spectra have the same shape.

Table 1: Overview of properties determined for the different detectors characterized in this work, together with a standard NaI detector as reference.

Crystal	Size (in. $\times$ in.)	Energy resolution for $^{137}\text{Cs}$	Intrinsic full peak efficiency for $^{137}\text{Cs}$	Intrinsic timing resolution for $^{60}\text{Co}$	Intrinsic activity (/cm $^3$ /s)
LaCl $_3$	1.5 $\times$ 1.5	4%	0.233(6)	398(5) ps	> 1.3
LaBr $_3$	2 $\times$ 2	2.9%	0.34(1)	338(8) ps	> 0.23
CeBr $_3$	1 $\times$ 1	4.4%	0.228(7)	326(7) ps	< 0.08
CeBr $_3$	1 $\times$ 2	4.4%	---	400(16) ps	< 0.03
NaI	3 $\times$ 3	7%	0.15	3 - 5 ns	---

response function for determination of mean energy and  $\gamma$ -ray multiplicity. Therefore, the next step in the analysis process is to investigate the behavior of the detectors relative to incoming energy. To do this we will use the Monte Carlo code Penelope [15] to simulate each detectors performance for energies up to 8 MeV.

#### 4. Summary and outlook

Table 1 summarizes all characteristic parameters obtained during our detector characterization. The properties of a LaBr $_3$  detector as well as of a NaI detector are included for comparison. After this extensive characterization of the different detectors we may conclude, that LaBr $_3$  and CeBr $_3$  are the two detector types that are best suited for the prompt fission  $\gamma$ -ray measurements we will perform in the future, the LaBr $_3$  detector because of the higher efficiency as well as the better energy resolution and the CeBr $_3$  detector for the lower intrinsic activity compared to the LaCl $_3$  detector.

In May 2012 we plan on setting up three CeBr $_3$  and two LaBr $_3$  detectors in a coincidence setup with a fission chamber containing  $^{235}\text{U}$  at the reactor in IKI Budapest. This setup will give us the opportunity to correlate prompt fission  $\gamma$ -rays with fission fragment properties.

#### References

- [1] K. S. Krane, Introductory Nuclear Physics, John Wiley & Sons, ISBN 0-471-80553-X (1987).
- [2] Nuclear Data High Priority Request List of the NEA (Req. ID: H3, H4).
- [3] SCIONIX Holland bv, P.O. Box 143, 3980 CC Bunnik, The Netherlands
- [4] <http://www.nudaq.com/download/DAQ2000/3B-2-5.pdf>
- [5] A. Oberstedt, S. Oberstedt, R. Billnert, W. Geerts, F.-J. Hambach, J. Karlsson, Nucl. Instr. and Meth. A 668 (2012) 14.
- [6] A. Owens, A.J.J. Bos, S. Brandenburg, C. Dathy, P. Dorenbos, S. Kraft, R.W. OStendorf, V. Ouspenski, F. Quarati, Nucl. Instr. and Meth. A 574 (2007) 110.
- [7] R. Nicolini, F. Camera, N. Blasi, S. Brambilla, R. Bassini, C. Boiano, A. Bracco, F. C. L. Crespi, O. Wieland, G. Benzoni, S. Leoni, B. Million, D. Montanati, A. Zalite, Nucl. Instr. Meth. A 582 (2007) 554.
- [8] J.K. Hartwell, R.J. Gehrke, Appl. Radiat. Isot. 63 (2005) 223.
- [9] M. Balcerzyk, M. Moszynski, M. Kapusta, Nucl. Instr. and Meth. A 537 (2005) 50.
- [10] P. Guss, M. Reed, D. Yuan, A. Reed, S. Mukhopadhyay, Nucl. Instr. and Meth. A 608 (2009) 297.
- [11] E. Andreotti, M. Hult, R. Gonzalez de Orduña, G. Marissens, M. Mihailescu, Status Proceedings of the 3rd International Conference on Current Problems in Nuclear Physics and Atomic Energy, 07–12 June 2010, Kiev, Ukraine, Publishing Department of KINR (Institute for Nuclear Research Kiev), accepted for publication, <<http://www.kinr.kiev.ua/NPAE-Kyiv2010/html/Proceedings/8/Andreotti.pdf>>.
- [12] R. Billnert, S. Oberstedt, E. Andreotti, M. Hult, G. Marissens, A. Oberstedt, Nucl. Instr. and Meth. A 647 (2011) 94.
- [13] G. Gilmore, Practical Gamma-ray Spectroscopy, John Wiley & Son, ISBN 978-0-470-86196-7 (2008).
- [14] G. F. Knoll, Radiation Detection and Measurement, John Wiley & Sons, ISBN 0-471-07338-5 (1999), Eq. 4.21.
- [15] <http://www.oecd-neo.org/tools/abstract/detail/nea-1525>.